Ciuncanu, M. and Chiroiu V., 2016. On the post-earthquake damage detection of structures. *Romanian Journal of Technical Sciences – Applied Mechanics, 61(3)*, pp.189–204.

ON THE POST-EARTHQUAKE DAMAGE DETECTION OF STRUCTURES

MIHAI CIUNCANU[1], VETURIA CHIROIU[2]

Abstract. The paper introduces an alternative method for evaluation the post-earthquake damage in the multidegree of freedom structures with viscous and hysteretic behavior. Assuming damage as a scalar variable is very simplistic. However, this simplification helps us to understand the damage as the failing which impairs functional and working conditions of engineering structures. The damage is computed from simulated data and the characteristics of the structures. The role of the strength and stiffness degradations in the damage evaluation is investigated, via extended Bouc-Wen model. The transition to damage as a vector variable is in progress.

Keywords: damage, earthquake, dissipated energy, hysteresis.

1. INTRODUCTION

In seismically active regions, such as Vrancea, the detection and quantification of the post-earthquake damage in structures is a challenge for structural engineers. The structural monitoring techniques are based on the vibration analysis data recorded on structures under dynamic excitations. The vibration data gathered by monitoring systems give useful information in the structural response and identification of the damage. In this context, the damage is an additional excitation which can modify the output signals. The Structural Health Monitoring (SHM) is usually tracking the damage by interpretation the changes that appear in measuring data so that the structural reability can be quantified [1–3]. The detection of damage is an inverse problem where measurable outputs are used to detect the damage. Kachanov proposed in 1958 a model of damage based on a dimensionless scalar variable ψ denoted continuity [4]. An undamaged material is described by $\psi = 1$, whereas $\psi = 0$ characterizes a completely destroyed material with no load carrying capacity. The complementary quantity $D = 1–\psi$ is therefore a measure

[1] Research Institute for Construction Equipment and Technology – ICECON, Bucharest
[2] Institute of Solid Mechanics of the Romanian Academy, Bucharest

of the state of deterioration of the material or damage. For $D=0$ the material is undamaged, whereas $D=1$ corresponds to the complete loss of the integrity of the material. The deterioration of the material is caused by microcracks and voids which decrease in load carrying area. For example, in the elongation of the beam the nominal stress is $\sigma_0 = P/A_0$ where A_0 denotes initial cross sectional area before the load is applied. The real stress is $\sigma = P/A$ where A denotes cross sectional area as defined by exterior cross sectional size. The effective stress is $s = \sigma/(1-D)$ where D is the damage parameter, according to Rabotnov) [5–7]. The effective stress can be rewritten as $s = P/[A(1-D)]$.

Consequently, the quantity $A(1-D)$ can be interpreted as a fictitious load carrying area, decreasing from A to 0. The value 0 means rupture or failure of the material. The damage law can be postulated as $\dot{D} = Cs^{\alpha}$ [8, 9], where C and s are experimentally obtained. We have for majority of metals $0.2 < D < 0.8$, according to Chaboche [10]. A single scalar damage parameter is often insufficient to describe the characteristics of damaged structures. For example, Murakami [11] described the microscopic mechanisms and features for each type of damage.

In this context, the generation and growth of microscopic cracks caused by elastic deformations and change of effective stiffness due to the strength reduction and elastic modulus drop characterize the elastic-brittle damage (metals, rocks, concrete, composites). The generation, growth and coalescence of microscopic voids caused by large elastic-plastic deformations characterize the elastic-plastic damage (metals, polymers, composites). The generation, growth of microscopic cracks in the vicinity of the surface, high cycle failure larger than 10^5 or very low cycle failure below 10, characterize the fatique damage. The generation and growth of microscopic voids and cracks in metal grains (ductile creep damage) or in intergranular boundaries (brittle damage) due to grain boundaries sliding and diffusion characterize creep damage.

The effect of earthquakes on the structures may be described by measured vibration response of the structure. The vibration response can be used as a diagnosis tool to assess the damage in structure. Various strategies have been proposed in this context [12–17].

The objective of this paper is to present an alternative method for evaluation the post-earthquake damage in the structures. The method is based on the dissipated energy. The energy can be dissipated during the earthquake as the frictional heat generation, or in defects. The amount of energy dissipated on damage is proportional to the amount of mechanical energy delivered to the structure. The role of the strength and stiffness degradations in the damage evaluation is investigated, via extended Bouc-Wen model.

A useful analytical description of the hysteretic behaviour was introduced by Bouc [18] and extended by Wen [19] via the following inverse problem: *given a set of experimental input-output data, how to adjust the Bouc-Wen model parameters so that the output of the model matches the experimental data*. Once the Bouc-Wen

model parameters are identified, the resulting model is considered as a *resonable approximation* of the real hysteresis when the error between the experimental data and the output of the model is small enough from practical point of view [20–23]. The genetic algorithms were widely used for curve fitting the Bouc-Wen model to experimentally obtained hysteresis loops [24–26].

2. SDOF WITH VISCOUS AND HYSTERETIC DAMPING

Let us begin with a SDOF structure subjected to base excitation

$$m\ddot{y} + c\dot{x} + R(x,z,t) = 0\,, \tag{1}$$

where x is the relative displacement, $\dot{x}$ is the relative velocity, $\ddot{y} = \ddot{x} + a_g$ is the absolute acceleration of the mass, a_g is the ground acceleration used to excite the model, m is the mass, $c\dot{x}$ is damping restoring force with c the damping coefficient, and $R(x,z,t)$ is the restoring force

$$R(x,z,t) = \alpha k x + (1-\alpha) k z\,, \tag{2}$$

which is a sum of the linear restoring force αkx and the hysteretic restoring force $(1-\alpha)kz$, where $0<\alpha<1$ is the rigidity ratio representing the relative participations of the linear and nonlinear terms [14]. The function $z(x,\dot{x})$ is the hysteretic auxiliary variable representing the hysteretic displacement function of the time history of x. It is related to $x(t)$ through the constitutive law the force-displacement [17, 27, 28]

$$\eta \frac{\mathrm{d}z}{\mathrm{d}x} = h(z)\Big(A - \nu(\beta\,\mathrm{sgn}(\dot{x}) \mid z \mid^{n-1} z + \gamma \mid z \mid^{n})\Big), \tag{3}$$

where $h(z)$ is the pinching function (for $h=1$ the function is not pinch), A a parameter that controls the tangent stiffness and ultimate hysteretic strength, β,γ,n are the hysteretic shape parameters and ν,η are the strength and stiffness degradation functions (for $\nu=\eta=1$ the model is not degrading). These functions depend on the dissipated hysteretic energy. The law (3) extends the Bouc-Wen model by including the pinching function. This equation originally driven in Baber's studies in 1981 to 1986 [29–32].

By setting $\mathrm{d}z/\mathrm{d}x$ to zero in (3) and solving it for z, we obtain the ultimate hysteretic strength z_u

$$z_u = \left(\frac{A}{\nu(\beta+\gamma)}\right)^{1/n}. \tag{4}$$

The pinching function $h(z)$ is taken under the form [16]

$$h(z)=1-\zeta_1\exp\{-(z\,\mathrm{sgn}(\dot{x})-z_u)^2/\zeta_2^2\}, \tag{5}$$

where $\zeta_1<1$ is a variable which controls the magnitude of initial drop in the slope $\mathrm{d}z/\mathrm{d}x$, and ζ_2 a variable which controls the rate of change of the slope $\mathrm{d}z/\mathrm{d}x$. The motion equations for SDOF are

$$m\ddot{y}+c\dot{x}+\alpha kx+(1-\alpha)kz=0, \tag{6}$$

$$\eta\frac{\mathrm{d}z}{\mathrm{d}x}=h(z)\Big(A-\nu(\beta\,\mathrm{sgn}(\dot{x})\,|\,z\,|^{n-1}\,z+\gamma\,|\,z\,|^{n})\Big). \tag{7}$$

In order to obtain an energy balance relationship, we multiply both equations (6) and (7) by $\frac{\mathrm{d}x}{\mathrm{d}t}\mathrm{d}t$ and integrate between the time t_1 from which the system starts to move from rest, and the time t_2 for which the system comes to rest after motion

$$m\int_{t_1}^{t_2}\dot{x}\ddot{y}\,\mathrm{d}t+c\int_{t_1}^{t_2}\dot{x}^2\mathrm{d}t+\alpha k\int_{t_1}^{t_2}\dot{x}x\,\mathrm{d}t+(1-\alpha)k\int_{t_1}^{t_2}\dot{x}z\,\mathrm{d}t=0, \tag{8}$$

$$\eta\int_{t_1}^{t_2}\dot{x}\frac{\mathrm{d}z}{\mathrm{d}x}\mathrm{d}t=\int_{t_1}^{t_2}\dot{x}\,h(z)\Big(A-\nu(\beta\,\mathrm{sgn}(\dot{x})\,|\,z\,|^{n-1}\,z+\gamma\,|\,z\,|^{n})\Big)\mathrm{d}t. \tag{9}$$

By noting the elastic strain energy stored between t_1 and t_2 with U

$$U=\alpha k\int_{t_1}^{t_2}\dot{x}x\,\mathrm{d}t=\alpha k\int_{x(t_1)}^{x(t_2)}x\mathrm{d}x, \tag{10}$$

the energy dissipated by hysteretic loops with E_{hys}

$$E_{hys}=(1-\alpha)k\int_{t_1}^{t_2}\dot{x}z\,\mathrm{d}t=(1-\alpha)k\int_{x(t_1)}^{x(t_2)}z\mathrm{d}x, \tag{11}$$

and the energy dissipated by viscous damping between t_1 and t_2 with E_{damp}

$$E_{damp}=c\int_{t_1}^{t_2}\dot{x}^2\mathrm{d}t. \tag{12}$$

Eqs. (8) and (9) become

$$m\int_{t_1}^{t_2}\dot{x}\ddot{y}\,\mathrm{d}t+E_{damp}+E_{hys}+U=0, \tag{13}$$

$$\int_{x(t_1)}^{x(t_2)}h(z)\Big(A-\nu(\beta\,\mathrm{sgn}(\dot{x})\,|\,z\,|^{n-1}\,z+\gamma\,|\,z\,|^{n})\Big)\mathrm{d}x=\eta(z(t_2)-z(t_1)). \tag{14}$$

When the system has coming to rest after moving, the strain energy U tends to zero, so from (12) we have

$$E_d = E_{damp} + E_{hys} = -m\int_{t_1}^{t_2} \dot{x}\ddot{y}\,\mathrm{d}t\,, \tag{15}$$

where E_d is the total dissipated energy.

In the spirit of [11] let us define the damage parameter $0 \le D < 1$ for SDOF as

$$D = \frac{E_{hys}}{E_d} = 1 - \frac{E_{damp}}{E_d} = 1 + \frac{c\int_{t_1}^{t_2} \dot{x}^2\mathrm{d}t}{m\int_{t_1}^{t_2} \ddot{y}\dot{x}\,\mathrm{d}t}, \tag{16}$$

where c is the damping constant and m is the mass. The damage parameter D always lies in the interval [0, 1]. When $E_{hys} = 0$ we have $E_d = E_{damp}$ and then D = 0 that means it is no damage, while $D_{damp} = 0$ leads to $D = 1$ which is a nonrealistic situation because the energy cannot be dissipated only through hysteretic loop. Some amount of energy always is dissipated through damping.

The damage parameter D is not appropriate for applications because the static damage component is not existing and therefore D cannot reflect very slow dependent of time load.

Actually, the definition (16) does not make explicit or implicit references to the stiffness of the structure, therefore it does not rely on extension of concepts such as natural frequency [12]. So, by dividing (1) by m, we obtain

$$\ddot{y} + 2\zeta_0\omega_0\dot{x} + \alpha\omega_0^2 x + (1-\alpha)\omega_0^2 z = 0\,, \tag{17}$$

where $\omega_0 = \sqrt{k/m}$ and $\zeta_0 = c/2\sqrt{km}$ is the damping ratio, and the damage parameter D can be rewritten as

$$D = 1 + \frac{4\pi\zeta_0\int_{t_1}^{t_2} \dot{x}^2\mathrm{d}t}{T\int_{t_1}^{t_2} \ddot{y}\dot{x}\mathrm{d}t} = 1 + \frac{2\zeta_0\omega_0\int_{t_1}^{t_2} \dot{x}^2\mathrm{d}t}{\int_{t_1}^{t_2} \ddot{y}\dot{x}\mathrm{d}t}, \tag{18}$$

where T is the fundamental period. Definition (18) is usually used for cases that do not exhibit a well-defined linear range before yielding.

The damage evaluation needs the signification of each unknown parameter $\{\alpha, A, \beta, \gamma, n, \zeta_1, \zeta_2\}$ and two unknown functions $\{\nu, \eta\}$ which describe the hysteretic phenomenon. In the following we will see that α, β, γ and n can be directly evaluated from the experiment, i.e. the restoring force against displacement. The system properties are evaluated from the model. The first natural frequency is calculated as $\sqrt{k/m}$, where m is the estimated mass of the system and k the initial stiffness.

The value of the linear damping ratio ξ_0 may be chosen within the range 0.01 and 0.05.

It was proved in [33] that A is redundant and, as a consequence, it is assumed to be 1. The parameter α is computed as

$$\alpha = \frac{k_f}{k_i}, \tag{19}$$

$$k_i = \left.\frac{\mathrm{d}R}{\mathrm{d}x}\right|_{z=x=0} = k, \quad k_f = \left.\frac{\mathrm{d}R}{\mathrm{d}x}\right|_{z=z_x} = \alpha k. \tag{20}$$

The equations for loading paths are obtained from (3) for $\nu = \eta = 1$ and $h = 1$

$$\frac{\mathrm{d}z}{\mathrm{d}x} = 1 - (\beta + \gamma) z^n, \quad z\dot{x} > 0, \tag{21}$$

and for unloading case

$$\frac{\mathrm{d}z}{\mathrm{d}x} = 1 - (\gamma - \beta) z^n, \quad z\dot{x} < 0. \tag{22}$$

The parameters β and γ are determined from (3) for $h = 1$ and $\nu = \eta = 1$ written under the form [17]

$$\frac{\mathrm{d}z}{\mathrm{d}x} = 1 - (\beta + \gamma) z^n, \quad z \geq 0, \ \dot{x} \geq 0, \tag{23}$$

$$\frac{\mathrm{d}z}{\mathrm{d}x} = 1 - (\gamma - \beta) z^n, \quad z \geq 0, \ \dot{x} < 0, \tag{24}$$

$$\frac{\mathrm{d}z}{\mathrm{d}x} = 1 + (-1)^{n+1} (\beta + \gamma) z^n, \quad z < 0, \ \dot{x} < 0, \tag{25}$$

$$\frac{\mathrm{d}z}{\mathrm{d}x} = 1 + (-1)^{n+1} (\gamma - \beta) z^n, \quad z \leq 0, \ \dot{x} \geq 0. \tag{26}$$

For non-degrading case $\nu = 1$, we obtain from (4) and (23)

$$\frac{\mathrm{d}z}{\mathrm{d}x} = 1 - \left(\frac{z}{z_x}\right)^n, \tag{27}$$

from which n can be determined. The shape parameters are chosen so that $\beta + \gamma > 0$ and $\gamma - \beta \leq 0$, with $\beta > 0$ in order to have a positive energy dissipation.

The stiffness and strength degradation functions ν and η are related to the dissipated hysteretic energy E_{hys} [16]

$$\nu(E_{hys}) = 1 + \delta_\nu E_{hys}, \quad \eta(E_{hys}) = 1 + \delta_\eta E_{hys}, \tag{28}$$

where E_{hys} is given by (11)

$$E_{hys} = \omega_0^2 \left(1 - \frac{k_f}{k_i}\right) \int_{t_1}^{t_2} z\dot{x}\,\mathrm{d}t, \quad 0 < \frac{k_f}{k_i} < 1. \tag{29}$$

The energy E_{hys} is the cumulative dissipated hysteretic energy, in other words the sum of the loops areas. The functions $\nu(E_{hys})$ and $\eta(E_{hys})$ control the strength and stiffness degradations. $\delta_\nu > 0$ and $\delta_\eta > 0$ are unknown parameters. The stiffness degradation occurs when the elastic stiffness degrades with increasing ductility, as shown in Fig. 1 left. This behavior occurs in damage patterns of the ductile behavior of structures to earthquakes. The strength degradation is described by reducing the capacity in the backbone curve, as shown in Fig. 1 right.

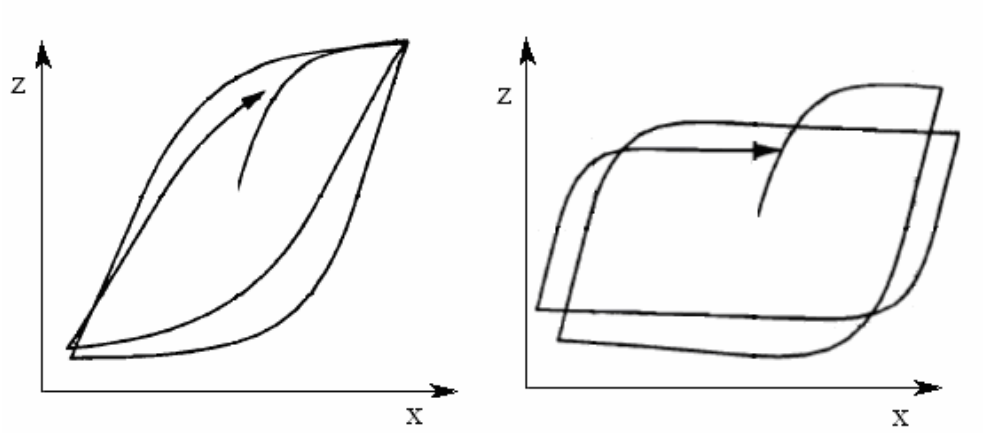

Fig. 1 – Left: stiffness degradation behavior; right: strength degradation behavior [17].

Figure 2 shows the pinching behavior in the diagram $\mathrm{d}z/\mathrm{d}x$ against z/z_u, where z_x is the ultimate hysteretic strength, given by (4). The pinching is the typical behavior of structures that buckle when subjected to compressive loads. This behavior usually is the result of cracks or slips.

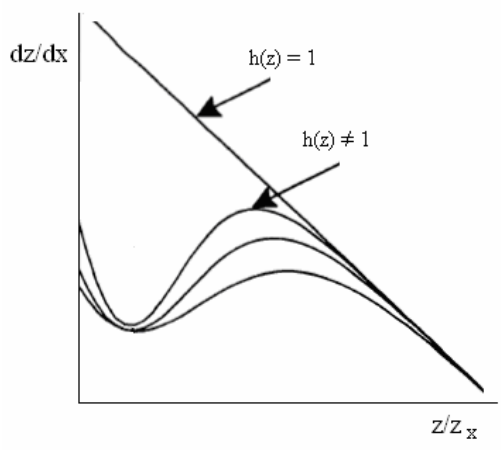

Fig. 2 – Pinching behavior for $h(z) \neq 1$ [17].

To identify the remaining parameters $\delta_v, \delta_\eta, \zeta_1$ and ζ_2, that cannot be directly evaluated from the experiment, a genetic algorithm can be applied in the same manners as in [24–27], by using experimental data. By using (16), the damage can be defined as

$$D = (1-\alpha)\left(\frac{E_{damp}}{E_{damp,mon}}\right)^{1/2} + \alpha\left(\frac{E_{hys}}{E_{hys,mon}}\right)^{1/2}, \tag{30}$$

where α must be chosen based on experiment and depends on the material. The E_{damp} is the energy dissipated by viscous damping defined by (12), $E_{damp,mon}$ is the monotonic energy due to the monotonic viscous dissipation capacity, and E_{hys} is the hysteretic energy dissipation capacity, and $E_{hys,mon}$ is the monotonic hysteretic energy dissipation capacity. The monotony refers to the monotonic loading. We see from (30) that *D* is zero if the response is linear, and is unity when the displacement capacity under monotonic loading is reached. This does not mean that *D* exceeds one under dynamic loading. Both definitions for the damage parameter *D*, (18) and (30) coincide at zero when the response is linear and will have to be mapped for nonlinear response for other values.

3. DAMAGE EVALUATION

In this example, the artificial ground acceleration a_g which excites the SDOF structure is displayed in Fig. 3. The characteristic period of ground motion is $T_g = 0.6$ s for a long epicentre distance. The structure period varies from 0.1 to

1.2 s with an increment of 0.1 s. The time t_1 from which the system starts to move from rest is $t_1 = 0$, and the time t_2 for which the system comes to rest after motion is considered $t_2 = 60$ s (50 periods). As we said before, the duration of seismically excitation is important. The longer the earthquake excitation, the more energy enters into the structure, thus more energy dissipates on damage. The damping ratio is $c = 0.05$. The hysteretic parameters are summarized in Table 1. The total input energy W_{in} [(cm/s)^2] is shown in Fig. 4. Each turning point in Fig. 4 approximately corresponds to T_g.

Table 1

The parameter values used in the numerical simulation

α	β	γ	n	ζ_1	ζ_2	δ_ν	δ_η
0.47	0.87	0.90	2.15	0.94	0.72	0.21	0.22

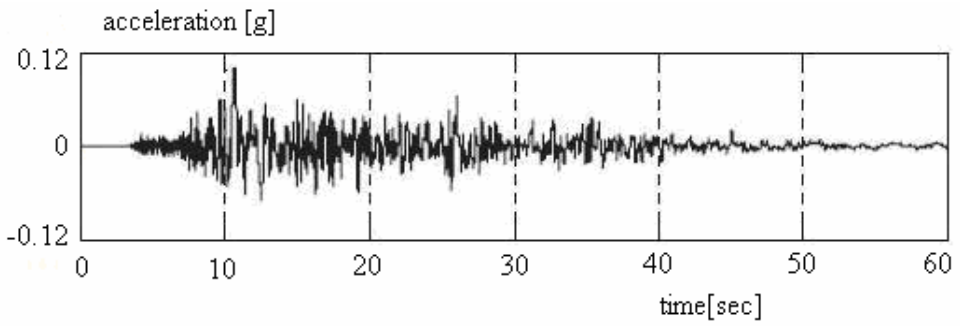

Fig. 3 – Ground acceleration used to excite the model.

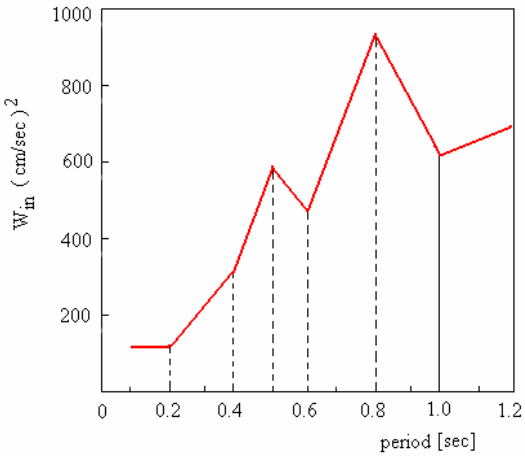

Fig. 4 – Total input energy.

The damage parameter is computed from (30) after solving the motion equations. The solution x and $\ddot{x}$ are presented in Figs. 5 and 6 by dotted lines, whereas the contribution of viscosity is shown by solid lines and the contribution of the hysteretic behavior by red lines, respectively.

Although the damage parameter does not depend on time, it is understandable that the damage is additive and cumulative over time. Cumulative damage can be computed on different interval of time during the seismically excitation. Cumulative damage after 60 s is presented in Fig.7.

According to Fig. 7, the damage parameter is additive and does not decrease. The damage level increases from $D=0.16$ to $D=0.38$ in 60 s. It is intuitively estimated and numerically confirmed that the average damage per unit of time is given by $\delta_\nu/3+\delta_\eta$. It corresponds to the value $D=0.03$.

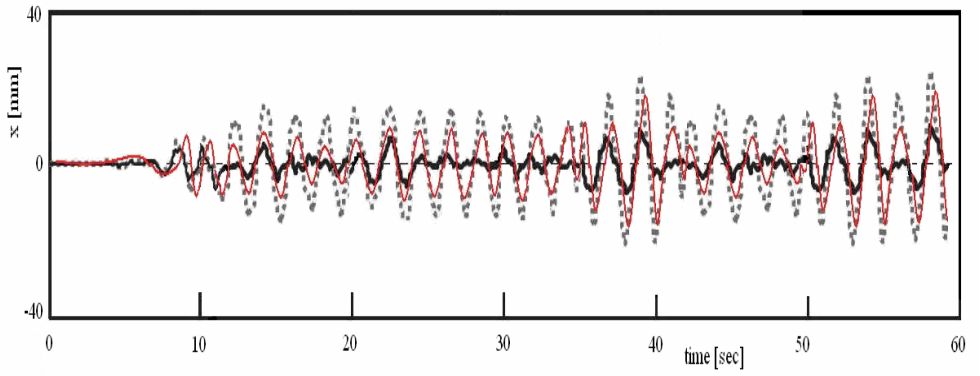

Fig. 5 – Displacement *x*: solution (dotted line), contribution of viscous (solid line) and hysteretic behavior (red), respectively.

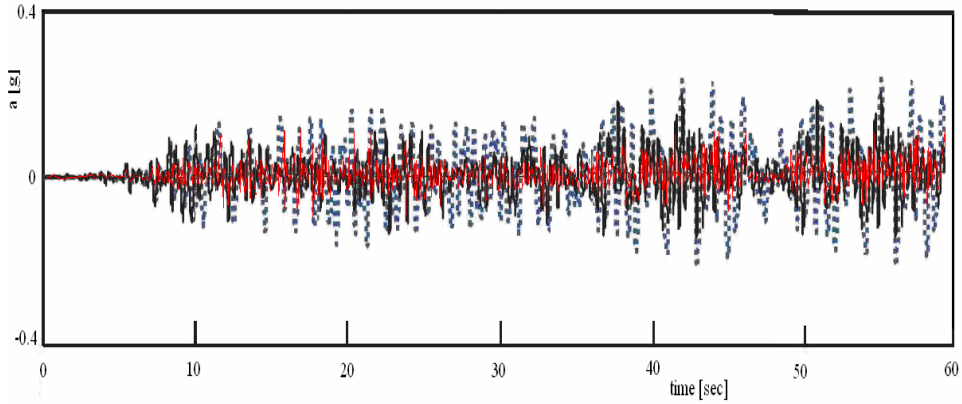

Fig. 6 – Flow acceleration: solution (dotted line) and contribution of viscous (solid line) and hysteretic behavior (red), respectively.

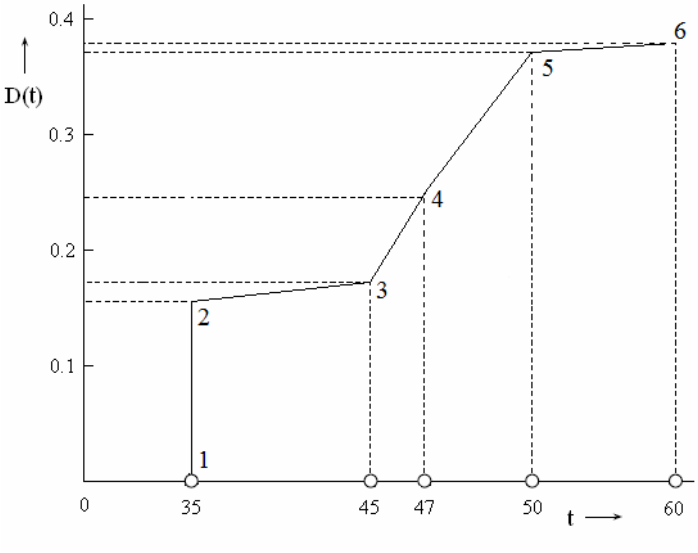

Fig. 7 – Cumulative damage for 5 moments of time.

The energy E_{damp} is represented in Fig. 8, for c = 0.05. The effect of viscous damping on the input energy is demonstrated. A larger damping ratio can remarkable reduce the input energy.

The energy E_{hys} is represented in Fig. 9. We observe that E_{hys} has a graphic with approximately parallel lines with the input energy lines shown in Fig. 4, and has similar shapes. The percentage of hysteretic energy in total input energy is approx. 37.5 % and is independent of structural period and ground motion.

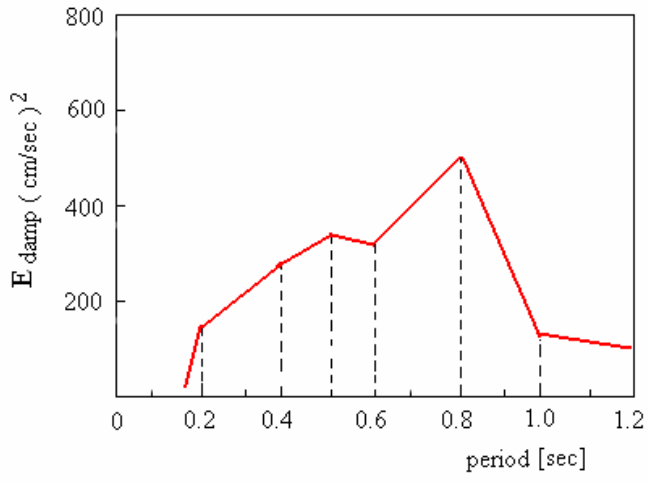

Fig. 8 – The energy dissipated by viscous damping for c = 0.05.

We know that cumulative damage leads to failure of the structure through material failure or through the structural instability. The material failure is independent of structural geometry and size. The structural instability depends on structural geometry and size and it is governed by the stiffness of the material.

Localization of high amplitudes solutions in certain interval of times as shown in Figs. 5 and 6 is related to the brittle damage of structures for which shear bands, plastic hinges and localized instabilities appear into the material. This damage localization problem is the foundation for local breakdown or failure.

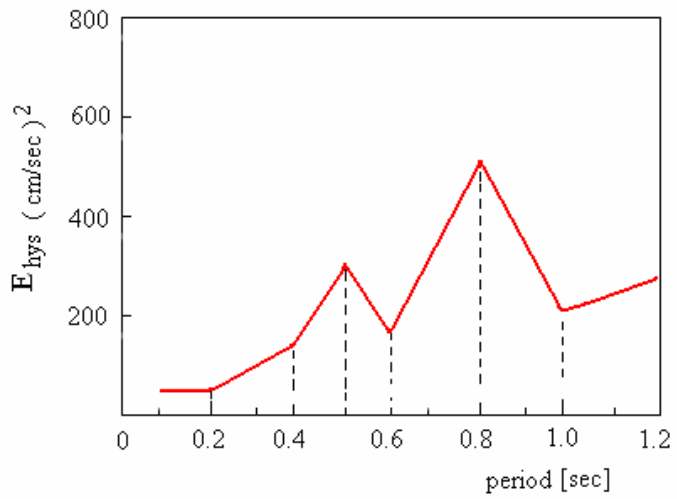

Fig. 9 – The energy dissipated by hysteresis behavior.

The stiffness and damage at each state represented in Fig. 7 for 5 moments of time, are shown in Table 2. We see that in severe damages, the reduction of stiffness is approximately 37–40%, while in the minor cases the reduction is approximately 22%.

Table 2

Stiffness and damage at each state

Moments of time	Stiffness [N/m]	Percentage of remaining stiffness
1	4.8×10^5	100
2	3.9×10^5	84
3	3.7×10^5	82
4	3.4×10^5	74
5	2.3×10^5	64
6	1.8×10^5	62

In the case of corrupted experimental data introduced during measurement, the hysteretic system is identified with simulated noisy data as

$$\bar{y}(t_i) = (1 + \varepsilon r_i) y(t_i), \tag{31}$$

where r_i is a sequence of random variables with a uniform distribution in the interval (–1, 1) and parameter ε is the noise to signal ratio. Identification results from noise-corrupted data are presented in Table 3 for α, β, γ and *n*. The parameters $\delta_\nu, \delta_\eta, \zeta_1$ and ζ_2, are determined from a genetic algorithm by using corrupted experimental data.

Table 3

The parameter values from corrupted data

α	β	γ	n	ζ_1	ζ_2	δ_ν	δ_η
0.472	0.872	0.906	2.155	0.943	0.726	0.209	0.218

The true parameter values are given in Table 1. The results of Table 2 demonstrate that the proposed scheme is insensitive to noise.

A similar analysis can be carried out for the evaluation of the damage for multi-degree of freedom structures [33, 34]. The general energy balance expression can be written as

$$\int_{t_1}^{t_2} \left(\dot{x}^{\mathrm{T}} M \ddot{y} + \dot{x}^{\mathrm{T}} C \dot{x} + \dot{x}^{\mathrm{T}} F_R \right) \mathrm{d}t = 0, \tag{32}$$

where $x, \dot{x}$ are the relative displacement and velocity vectors, $\dot{y}$ the absolute mass velocity vector, *M*,*C* the mass and damping matrices, and F_R the restoring force vector.

Similarly to (16), we can write

$$D = \frac{E_{hys}}{E_d} = 1 - \frac{E_{damp}}{E_d} = 1 + \frac{\int_{t_1}^{t_2} \dot{x}^{\mathrm{T}} C \dot{x} \, \mathrm{d}t}{\int_{t_1}^{t_2} M \ddot{y} \dot{x} \, \mathrm{d}t}. \tag{33}$$

The *x* and *C* are not known and their estimation must be carefully performed in order to include the threshold of damage initiation and attainment of the critical strength. A disadvantage of this model is that it cannot be applied to complex structures where micro-damages and crack distribution in earthquake-damaged areas are essential for a real damage evaluation. For these cases, the continuum damage approach must be applied through the concept of fabric tensors in the frame of the viscoelasticity theory. Kachanov [4] introduced the theory of continuum damage for the isotropic case of uniaxial tension. Rabotnov [5] modified this theory for the case of creep. The damage

variable is interpreted in their works as the effective surface density of micro-damages per unit volume. A fictitious undamaged configuration of the body is considered and by comparing it with actual earthquake-damaged configuration, the damage constitutive equations are obtained. The concept of fabric tensor has been introduced by Kanatani [35] to describe directional data and microstructural anisotropy in damaged areas. Fabric tensors are further elaborated by Lubarda and Krajcinovic [36] to describe crack distributions in damaged structures.

4. CONCLUSIONS

An alternative method for evaluation the post-earthquake damage in the SDOF structures with viscous and hysteretic behavior is presented. The method is based on the dissipated energy. Assuming damage as a scalar variable is very simplistic. However, this simplification helps us to understand the damage as the failing which impairs functional and working conditions of engineering structures. Damage can also be regarded as a modification to material properties and/or structural physical parameters.

The proposed damage parameter depends on the ratio of the dissipated energy by means of hysteresis and the total dissipated energy. The Bouc-Wen model is modified in order to include the experimentally observed characteristics such as the stiffness and strength degradation and pinching, respectively. The damage parameter is computed from simulated data and the characteristics of the structure. Although the damage formula does not depend on time, it is understandable that the damage is additive and cumulative over time. Cumulative damage can be computed on different interval of times during the seismically excitation. The total damage increases in time. Cumulative damage is done through material failure or through the structural instability. The damage localization is of interest to the mechanics of earthquakes because the localization leads to incapability of the structure to transmit further the energy.

In general, the proposed method is not particularly sensitive to noise as demonstrated by corrupted data.

The problem treated in this paper considers that the damage is a scalar. For real applications under realistic conditions and real instrumented structures, it is necessary to treat the damage as a vector or a second-rank, fourth-rank or eighth damage tensors.

Acknowledgements. This research was elaborated through the PN-II-PT-PCCA-2011-3.1-0190 Project nr. 149/2012 of the National Authority for Scientific Research (ANCS, UEFISCSU), Romania. The authors acknowledge the similar and equal contributions to this article.

Received on August 31, 2016

REFERENCES

1. AKTAN, A.E., CATBAS, F.N., GRIMMELSMAN, K., PERVIZPOUR, M., CURTIS, J., SHEN, K., QIN, X., *Health monitoring for effective management of infrastructure*, SPIE's 9th Annual International Symposium on Smart Structures and Materials, The International Society for Optical Engineering, San Diego, CA, United States, 2002, pp. 17–29.
2. DEMETRIOU, M.A., HOU, Z. *On-line fault/damage detection schemes for mechanical and structural systems*, Journal of Structural Control, **10**, *1*, pp. 1–23, 2003.
3. DOEBLING, S.W., FARRAR, C.R., PRIME, M.B., SHEVITZ, D.W., *Damage identification and health monitoring of structural and mechanical systems from changes in their vibration characteristics*: *A literature review*, Los Alamos National Laboratory, 1996.
4. KACHANOV, L.M., *On the time to failure under creep conditions*, Izv. Akad. Nauk. SSSR, Otd. Tekhn., **8**, pp. 26–31, 1958.
5. RABOTNOV, Y.N., *Damage from creep* (in Russian), Zhurn. Prikl. Mekh. Tekhn. Phys., **2**, pp. 113–123, 1963.
6. RABOTNOV, Y.N., *On the mechanism of delayed fracture*, Izd. Akad. Nauk SSSR, Moscow, pp. 5–7, 1959.
7. RABOTNOV, Y.N., *Selected works. Problems of solid mechanics*, Nauka, Moscow, 1991.
8. KRAJCINOVIC, D., LEMAITRE, J. (eds.), *Continuum damage mechanics. Theory and applications*, Springer Verlag, 1987.
9. SKRZYPEK, J.J., GANCZARSKI, A., *Modeling of material damage and failure of structures*. *Theory and applications*, Springer Verlag, 1994.
10. CHABOCHE, J.L., *Continuum damage mechanics. Part I: General concepts, Part II: Damage growth, crack initiation, and crack growth*, J. Appl. Mech., **55**, *3*, pp. 59–71, 1988.
11. MURAKAMI, S., *Failure criteria of structured media*, Ed. A.A. Balkema, 1986.
12. HERNANDEZ, E.M., MAY, G., *Post-earthquake damage detection in instrumented buildings using identified dissipated energy* (Ch. 35), in: *Topics in Modal Analysis II* – Vol. 6, Conference Proceedings of the Society for Experimental Mechanics, Series 31, Springer New York, 2012, pp. 351–358.
13. LYNCH, J.P., WANG, Y., LU, K.C., HOU, T.C., LOH, C.H., *Post-seismic damage assessment of steel structures instrumented with self-interrogating wireless sensors*, Proceedings of the 8th National Conference on Earthquake Engineering, San Francisco, 2006.
14. BOZORGNIA, Y, BERTERO, V., *Damage spectra: characteristics and applications to seismic risk reduction*, ASCE J. Struct. Eng., **129**, *10*, 1330–1340, 2003.
15. MAU, S.T., RIVADIGAR, S., *Detecting structural damage from building seismic records*, Proceedings of the 5th U.S. National Conference on Earthquake Engineering, Oakland, pp. 331–340, 1994.
16. BERNAL, D., HERNANDEZ, E., *A data-driven methodology for assessing impact of earthquakes on the health of building structural systems*, The Structural Design of Tall and Special Buildings, **15**, *1*, pp. 21–34, 2006.
17. BOUC, R., *Forced vibration of mechanical systems with hysteresis*, Proc. Fourth Conf. Non-Linear Oscil., Prague, Czechoslovakia, 1967.
18. WEN, Y.K., *Method for random vibration of hysteretic systems*, J. Eng. Mech. Division, **102**, *2*, pp. 249–263, 1976.
19. SIRETEANU, T., GIUCLEA, M., MITU, A.M., *Identification of an extended Bouc-Wen model with application to seismic protection through hysteretic devices*, Computational Mechanics, **45**, *5*, pp. 431–441, 2010.
20. SIRETEANU, T., GIUCLEA, M., MITU, A.M., *An analytical approach for approximation of experimental hysteretic loops by Bouc-Wen model*, Proc. of Ro. Acad., Series A, **10**, *1*, 2009.
21. SIRETEANU, T., GIUCLEA, M., SERBAN, V., *Dynamic behaviour of structures with hysteretic characteristics. Application to seismic engineering* (Ch. 14), in: R*esearch Trends in Mechanics* – Vol. 4, Editura Academiei Române, Bucharest, 2010, pp. 321–348.

22. SIRETEANU, T., STOIA, N., *Vibration amplification in oscillating systems with degrading characteristics*, Rev. Roum. Sci. Techn. – Méc. Appl., **53**, *1*, pp. 75–84, 2008.
23. SIRETEANU, T, GIUCLEA M., *A genetic algorithm method for synthesizing seismic accelerograms*, Proc. Ro. Acad., Series A, **1**, *1*, pp. 37–40, 2000.
24. GIUCLEA, M., SIRETEANU, T., MITU, A.M., *On the fitting of Bouc-Wen model by genetic algorithms*, Rev. Roum. Sci. Techn. – Méc. Appl., **54**, *1*, pp. 3–10, 2009.
25. SIRETEANU, T., GIUCLEA, M., MITU, A.M., GHITA, G., A *Genetic Algorithms Method for fitting the generalized Bouc-Wen model to experimental asymmetric hysteretic loops*, ASME Journal of Vibration and Acoustics, **134**, *4*, p. 041007, 2012.
26. GIRIP, I., DONESCU, ST., POIENARIU, M., MUNTEANU, L., *On the behaviour of the hysteretic wire-rope isolators under random excitation*, Rom. J. Techn. Sci. – Applied Mechanics, **58**, *3*, pp. 209–221, 2013.
27. GIRIP, I., MUNTEANU, L. GLIOZZI, A., *Inverse problems in the hysteresis modeling* (Ch. 5), in: *Inverse Problems and Computational Mechanics* – Vol. 1 (eds. L. Marin, L. Munteanu, V. Chiroiu), Editura Academiei Române, Bucharest, 2011, pp. 125–146.
28. BABER, T.T., WEN, Y.K., *Random vibrations of hysteretic degrading systems*, ASCE Journal of Engineering Mechanics, **107**, *6*, pp. 1069–1089, 1981.
29. BABER, T.T., NOORI, M.N., *Random vibration of degrading pinching systems*, ASCE Journal of Engineering Mechanics, **111**, *8*, pp. 1010–1026, 1985.
30. BABER, T.T., NOORI, M.N., *Modeling general hysteresis behaviour and random vibration applications*, Journal of Vibration, Acoustics, Stress, and Reliability in Design, **108**, *4*, pp. 411–420, 1986.
31. WEN, J.F., TU, S.T., GAO, X.L., REDDY, J.N., *Simulation of creep crack growth in 316 stainless steel using a novel creep-damage model*, Engineering Fracture Mechanics, **98**, pp. 169–184, 2013.
32. STAMMERS, C.W., SIRETEANU, T., *Control of building seismic response by means of three semi-active friction dampers*, Journal of Sound and Vibration, **273**, *5*, pp. 745–759, 2000.
33. CHOI, H., SANADA, Y., KASHIWA, H., WATANABE, Y., TANJUNG, J., JIANG, H., *Seismic response estimation method for earthquake-damaged RC buildings*, Earthquake Engng. Struct. Dyn., 45, pp. 999–1018, 2016.
34. YEONGAE, H., KUNNATH, S.K., *Damage-based seismic performance evaluation of reinforced concrete frames*, Int. J. of Concrete Structures and Materials, **7**, *3*, pp. 175–182, 2013.
35. KANATANI, K.-I., *Distribution of directional data and fabric tensors*, Int. J. Engng. Sci., **12**, *2*, pp. 149–164, 1984.
36. LUBARDA, V., KRAJCINOVIC, D., *Damage tensors and the crack density distribution*, Int. J. of Solids and Structures, **30**, *20*, pp. 2859–2877, 1993.